Experimental and numerical study of pulverized lignite combustion in air and oxy-fuel conditions

Halina Pawlak-Kruczek[1], Robert Lewtak[*, 2], Michał Ostrycharczyk[1]

[1] Department of Mechanical and Power Engineering, Wrocław University of Technology
[2] Department of Thermal Processes, Institute of Power Engineering, Warsaw, Poland

Abstract

The oxy (at the 25% and 30% O_2 mole fraction) and air combustion of pulverized lignite was experimentally studied in a drop tube furnace operating at temperature of 1200°C. Profiles of main and trace species, temperature and coal burnout were measured. A new combustion model of pulverized coal has been developed and implemented into FLUENT code. The numerical results, including NO emission, show good agreement between experimental and numerical data so that the model can be further applied to simulate pulverized coal combustion in industrial devices.

Introduction

Since the oxy combustion technology still seems to be a promising method for reduction of the CO_2 emission coming from power plants burning fossil fuels, all aspects connected with this new technology should be carefully studied before industrial implementation. Thus, fundamental research, including experimental tests, mathematical modelling and numerical simulations, should be first carried out to understand the complex combustion process. This paper, dealing with the basic research, increases understanding of the subject by laboratory experiments and numerical study.

Experimental setup

Laboratory combustion experiments of pulverized lignite, from Polish Turów coal mine, were carried out in an isothermal flow reactor of 20 kW thermal power. The reactor, presented in Fig. 1, consists of a vertical 3-meter ceramic cylindrical tube of the 135-mm inner diameter and electrically heated up to 1200°C [1].

The reactor burner, composed of two separate inlets and partially installed inside the tube, supplied predried (15% moisture) pulverized lignite with the carrying primary gas (80°C, 1.5 m^3/h) through the central path into the reactor. The secondary gas (120°C, 2.5 m^3/h) was supplied into the reactor by the outer ring of the burner equipped with a diffusor. The residence time of fuel in the reactor was up to 2 s. The measurements of O_2, CO, NO, SO_2 mole fractions were performed using infrared spectroscopy (Servomex and FT-IR equipment) and paramagnetic analyser (Oxymat61). The measurement points were located at the reactor axis at 6 different distances of 56 cm, 95 cm, 135 cm, 215 cm, 270 cm and 310 cm from the reactor top.

Three different combustion atmospheres were used to burn pulverized lignite at 1200°C. The first one was air and the others were two mixtures consisting of the 25% and 30% O_2 mole fraction with CO_2 as the rest gas. The excess O_2 ratio varied from 1.30 for oxy and 1.45 for air combustion. Under the reactor, the two-stage system of ash collection was installed with the quenching probe. Additionally, the two tests of pulverized lignite devolatilization were carried out in pure N_2 and CO_2 at 1000 °C to get lignite char for further analysis.

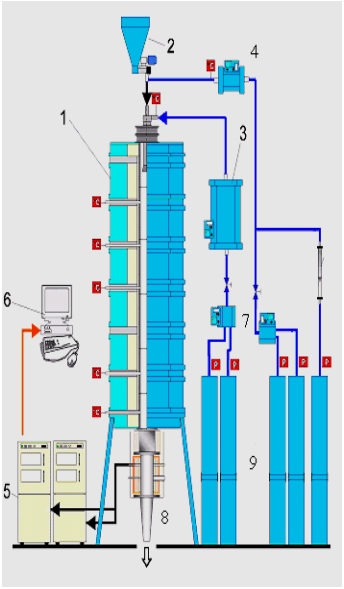

Fig. 1: Scheme of the experimental facility (1 reactor, 2 feeder, 3 secondary gas stream heater, 4 carrying gas stream heater, 5 FT-IR and Oxymat 61 analyzer, 6 controlling unit, data archiving, 7 gas mixers, 8 cooling unit, 9 gas batteries)

Table 1: Proximate and ultimate analysis of lignite and lignite char formed in N_2 and CO_2

component:	lignite	char N_2	char CO_2
moisture, %	14.10	1.86	1.57
ash, %	11.25	32.48	34.5
volatiles, %	49.36	0.0	0.0
combustible,%	74.65	65.70	63.90
HHV, kJ/kg	19870		
LHV, kJ/kg	18583		
C, %	45.53	62.47	60.55
H, %	4.32	0.70	0.87
O, %	23.11	0.47	0.57
N, %	0.44	0.52	0.43
S, %	1.25	1.51	1.53

Figure 2 shows the cumulative particle volume distribution based on the sieve analysis of pulverized lignite. The particle distribution has been estimated by the Rosin-Rammler distribution:

$$Y_{RR} = e^{-(d/\bar{d})^n} \quad (1)$$

with the parameters of n = 3.60 and $\bar{d}$ = 120 μm.

* corresponding author: robert.lewtak@ien.com.pl

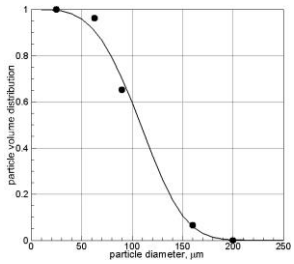

Fig. 2: Particle volume distribution based on the sieve analysis, • measured points, −Rosin-Rammler distribution

Combustion model

Combustion of pulverized coal is a complex process consisting of several overlapping or successive processes nonlinearly coupled, i.e. moisture evaporation, devolatilization, volatile matter and char combustion. The sequence of the above processes mainly depends on the coal type, the particle size and the particle heating rate.

In the current study, the Euler-Lagrange approach is applied to simulate combustion of pulverized lignite, i.e. the gas phase is treated in the Eulerian manner while the lignite particles are treated as Lagrange discrete particles moving in the gas phase. Both continuous and discrete phases interact with each other by exchange of mass, momentum and energy.

The key point of the combustion model is the composition of fuel. Based on the ultimate and proximate analysis of lignite and its char, the composition of the fuel particle has been defined as follows:

lignite = moisture + ash + volatiles + char = 100%, (2)

where volatiles, released during devolatilization, are represented in the following form:

$$\text{volatiles} = C_mH_nO_l + S_{(vm)} + N_{(vm)}, \quad (3)$$

in which the hydrocarbon, $C_mH_nO_l$, stands for all volatiles without sulfur and nitrogen compounds which are released as adequate compounds containing sulfur and nitrogen in the amount of $S_{(vm)}$ and $N_{(vm)}$, respectively. The char composition is as follows:

$$\text{char} = C_{(s)} + H_{(s)} + O_{(s)} + S_{(s)} + N_{(s)} \quad (4)$$

in which $C_{(s)}$, $H_{(s)}$, $O_{(s)}$, $S_{(s)}$ and $N_{(s)}$ stand for carbon, hydrogen, oxygen, sulfur and nitrogen which create a fixed combustible substance of lignite formed after devolatilization. Table 2 shows the lignite composition which has been applied in numerical simulations. The empirical formula of the released hydrocarbon is $C_{1.5}H_{2.82}O$ and its standard state enthalpy is 50.1 kJ/mol. Usually, coal moisture evaporation is the first step preceding pulverized coal combustion. Since evaporation is not a critical process requiring detailed investigation in the current study, it is modeled as a simple reaction

$$\text{moisture} \rightarrow H_2O_{(g)} \quad (5)$$

so that the evaporation rate is expressed as

$$r_{dry} = A_{dry}\, m_w\, e^{-E_{dry}/(RT_p)}, \quad (6)$$

where m_w is moisture mass remained in the particle, T_p is the particle temperature, A_{dry} = 300 1/s, E_{dry} = 17.0 kJ/mol. Also, devolatilization is treated in a simple way and described as following reactions

$$C_mH_nO_{l(s)} \rightarrow C_mH_nO_{l(g)} \quad (7)$$

$$S_{(vm)} \rightarrow H_2S_{(g)} \quad (8)$$

$$N_{(vm)} \rightarrow a\ HCN_{(g)} + (1 - a)\ NH_{3(g)} \quad (9)$$

that the devolatilization rate of $C_mH_nO_l$ is expressed as

$$r_{dev} = A_{dev}\, m_V\, e^{-E_{dev}/(RT_p)}, \quad (10)$$

where m_V is $C_mH_nO_l$ mass remained in the particle, $A_{dev} = 1\times10^5$ 1/s, E_{dev} = 132 kJ/mol. Since H_2S, HCN and NH_3 are released during devolatilization like $C_mH_nO_l$, their devolatilization rates are proportional to the devolatilization rate of $C_mH_nO_l$. The division of fuel nitrogen among HCN and NH_3 is described by the parameter of a whose value of 0.7 has been applied in numerical simulation.

Table 2: Composition of pulverized lignite

lignite component:	combustion in air	combustion in oxy-fuel
moisture, %	14.10	14.10
ash, %	11.25	11.25
volatiles, %, i.e.:	51.91	53.80
$C_mH_nO_l$, %	50.92	52.75
$N_{(vm)}$, %	0.26	0.30
$S_{(vm)}$, %	0.73	0.76
char, %, i.e.:	22.74	20.85
$C_{(s)}$, %	21.64	19.74
$H_{(s)}$, %	0.24	0.28
$O_{(s)}$, %	0.16	0.18
$N_{(s)}$, %	0.18	0.14
$S_{(s)}$, %	0.52	0.50

Char combustion consists in oxidation and gasification. The following oxidation reactions of char carbon

$$C_{(s)} + 0.5\ O_2 \rightarrow CO \quad (11)$$

$$C_{(s)} + O_2 \rightarrow CO_2 \quad (12)$$

play the major role in combustion. Other surface reactions, especially gasification reactions

$$C_{(s)} + CO_2 \rightarrow 2\ CO \quad (13)$$

$$C_{(s)} + H_2O \rightarrow CO + H_2, \quad (14)$$

oxidation of hydrogen, sulfur and nitrogen

$$H_{(s)} + 0.25\ O_2 \rightarrow 0.5\ H_2O \quad (15)$$

$$S_{(s)} + O_2 \rightarrow SO_2 \quad (16)$$

$$N_{(s)} + 0.5\ O_2 \rightarrow NO, \quad (17)$$

and the NO reduction reaction

$$C_{(s)} + NO \rightarrow CO + 0.5\ N_2, \quad (18)$$

play a minor role during air and oxy combustion.

It can be shown by employing the single film model that the oxidation rate of char carbon is expressed as

$$r_{C,i} = \pi d_p^2 M_C \psi_i \frac{k_d k_{c,i} f_s(X_C)}{k_d + f_s(X_C)(k_{c,1} + k_{c,2})} C_{O_2,\infty}, \quad (19)$$

with i = 1 for Eq (11) and i = 2 for Eq (12), ψ_1 = 2 mol-C/mol-O_2 and ψ_2 = 1 mol-C/mol-O_2, M_C = 12 kg/kmol,

$$k_d = \text{Sh}\ D / d_p \quad (20)$$

is the mass transfer coefficient, and the effective diffusion coefficient is defined as [2, 3]:

$$D(T) = D_0\,(0.5(T_{f,\infty} + T_p(t))/T_0)^{1.75}, \quad (21)$$

the rate coefficient of the i-th reaction is defined as

$$k_{c,i} = A_i\, e^{-E_i/(RT_s)} \quad (22)$$

where A_i and E_i are the kinetic parameters. The f_s function describes evolution of the specific surface area and the effect of the nonreactive ash surface during the coal particle combustion. In the current study, f_s gets the following form:

$$f_s(X_C) = (1 - X_C(t))^q, \quad (23)$$

where q = 1.65 [4], and

$$X_C(t) = (m_{C,0} - m_C(t))/m_{C,0} \quad (24)$$

is char carbon burnout.

For char carbon oxidation reactions Eqs. (11) and (12), the values of the kinetic parameters are coupled each other so that mole amount of CO and CO_2, formed in these reactions, satisfy the following expression:

$$p = \frac{\#\mathrm{CO}}{\#\mathrm{CO_2}} = A e^{-E/(RT)}\,, \tag{25}$$

where $A = 2A_1/A_2 = 70$ and $E = E_1\text{-}E_2 = 25.5$ kJ/mol [5] with $A_1 = 6700$ m/s and $E_1 = 76.0$ kJ/mol have been applied in the numerical simulations. The rate of gasification reactions Eqs. (13) and (14) is expressed as

$$r_{\mathrm{C},i} = \pi d_p^2\, M_{\mathrm{C}}\, \psi_i\, k_{c,i}\, f_s(\mathrm{X_C})\, C_{g,\infty}\,, \tag{26}$$

with $g = CO_2$ for $i = 3$ or $g = H_2O$ for $i = 4$, $\psi_3 = 1\mathrm{mol_C/mol_{CO2}}$, $\psi_4 = 1\mathrm{mol_C/mol_{H2O}}$, $C_{g,\infty}$ is mole concentration of the g-th species in the gas bulk, and $A_3 = A_4 = 2.55\times10^6$ m/s, $E_3 = 214$ kJ/mol, $E_4 = 180$ kJ/mol.

Since hydrogen, sulfur and nitrogen fixed in char are simultaneously oxidized during char carbon oxidation, their oxidation rates are proportional to the rate of char carbon oxidation. The rate of the NO reduction heterogeneous reaction (18) is expressed as

$$r_{\mathrm{C}} = \pi d_p^2\, M_{\mathrm{C}}\, \psi\, A\, e^{-E/(RT_s)}\, f_s(\mathrm{X_C})\, C_{\mathrm{NO},\infty}\,, \tag{27}$$

where A=8.9×10^4 m/s, E=133 kJ/mol, $\psi = 1\,\frac{\mathrm{mol_C}}{\mathrm{mol_{NO}}}$.

Gas phase combustion is dominated by oxidation of the main gas species:

$$\mathrm{C}_m\mathrm{H}_n\mathrm{O}_l + \tfrac{1}{2}(m + \tfrac{n}{2} - l)\,\mathrm{O_2} \rightarrow m\,\mathrm{CO} + \tfrac{n}{2}\,\mathrm{H_2O}\,, \tag{28}$$

$$\mathrm{CO} + 0.5\,\mathrm{O_2} \rightarrow \mathrm{CO_2} \tag{29}$$

$$\mathrm{H_2} + 0.5\,\mathrm{O_2} \rightarrow \mathrm{H_2O} \tag{30}$$

whose reaction rate, R_i, is defined by the finite rate/ eddy dissipation model as

$$R_i = \min(R_t, R_k)\,, \tag{31}$$

where R_t is the mixing rate defined for nonpremixed combustion as [6, 7]:

$$R_t = 23.6\left(\frac{\mu\varepsilon}{\rho k^2}\right)^{0.25} \frac{\rho}{M_{fu}}\,\frac{\varepsilon}{k}\,\min\left(Y_{fu}, \frac{Y_{ox}}{r}\right) \tag{32}$$

where values of ε and k are determined by a turbulence model adequate for the flow state. The Arrhenius rate is separately defined for each reaction, i.e. for Eq. (28) as

$$R_k = A\, e^{-E/(RT)}\, C_{vm}^{0.7}\, C_{\mathrm{O_2}}^{0.8} \tag{33}$$

where $A = 2.24\times10^{12}$, $E = 210$ kJ/mol, for Eq. (29) as

$$R_k = A\, e^{-E/(RT)}\, C_{\mathrm{CO}}\, C_{\mathrm{O_2}}^{0.25}\, C_{\mathrm{H_2O}}^{0.5} \tag{34}$$

where $A = 2.24\times10^{12}$, $E = 170$ kJ/mol, and for Eq(30) as

$$R_k = A\, e^{-E/(RT)}\, C_{\mathrm{H_2}}\, C_{\mathrm{O_2}} \tag{35}$$

where $A = 9.87\times10^8$, $E = 31.0$ kJ/mol, and the unit of A is so defined that $[R_k]$ = kmol/(s×m^3).

For the gas phase, the NO_x emission model consists of thermal, prompt and fuel mechanisms. The extended Zeldovich mechanism, describing the thermal NO_x formation, is reduced to one following reaction

$$\mathrm{N_2} + \mathrm{O_2} \rightarrow 2\,\mathrm{NO} \tag{36}$$

and the prompt NO formation path is defined as

$$\mathrm{C}_m\mathrm{H}_n\mathrm{O}_l + \mathrm{N_2} \rightarrow m\,\mathrm{HCN} + \ldots \tag{37}$$

in which nitrogen mainly comes from air and whose rate equations and parameters can be found in [8].

HCN and NH_3, released during lignite devolatilization, and NO, formed by oxidation of char nitrogen, evolve according to the De Soete model [9, 8]:

$$\mathrm{HCN} + 1.25\,\mathrm{O_2} \rightarrow \mathrm{NO} + \mathrm{CO} + 0.5\,\mathrm{H_2O} \tag{38}$$

$$\mathrm{HCN} + 1.5\,\mathrm{NO} \rightarrow 1.25\,\mathrm{N_2} + \mathrm{CO} + 0.5\,\mathrm{H_2O} \tag{39}$$

$$\mathrm{NH_3} + 1.25\,\mathrm{O_2} \rightarrow \mathrm{NO} + 1.5\,\mathrm{H_2O} \tag{40}$$

$$\mathrm{NH_3} + 1.5\,\mathrm{NO} \rightarrow 1.25\,\mathrm{N_2} + 1.5\,\mathrm{H_2O} \tag{41}$$

whose reaction rate equations and parameters can be found in [9, 8, 10, 11]. The NO can be also reduced by the homogeneous reburning reaction of

$$\mathrm{C}_m\mathrm{H}_n\mathrm{O}_l + \mathrm{NO} \rightarrow m\,\mathrm{HCN} + \ldots \tag{42}$$

whose reaction rate equation and parameters can be found in [12].

Although the SO_x emission has been taken into account in the current combustion model and numerical simulations as well, no detailed reactions describing SO_x model have been presented in the current study in which the combustion process and the NO_x emission were the main topic to discuss.

Finally, the particle conservation equations of mass and energy can be presented. The mass conservation equation of the i-th particle component is defined as

$$\frac{dm_{i,p}}{dt} = -r_{i,p} \tag{43}$$

where $m_{i,p}$ is mass of the i-th particle component decreasing in corresponding rate of $r_{i,p}$, and the total particle mass is expressed as follows

$$m_p(t) = \textstyle\sum_i m_{i,p}\,. \tag{44}$$

Each i-th Eq. (43) is solved with the initial condition of

$$m_{i,p}(0) = f_{i,0}\, V_{p,0}\, \left(\sum_i \frac{f_{i,0}}{\rho_i}\right)^{-1}\,, \tag{45}$$

where $f_{i,0}$ is the initial mass fraction of the i-th particle component having true density of ρ_i, $V_{p,0} = \frac{\pi}{6} d_{p,0}^3$ is the initial particle volume. Evolution of the particle volume is described as

$$V_p(t) = V_{p,0}(1 - \mathrm{X}_p)^{\alpha} \tag{46}$$

where α = 1.0 [13,14], X_p is the total particle burnout. Next, the particle density is determined as

$$\rho_p(t) = \frac{m_p(t)}{V_p(t)}\,. \tag{47}$$

Thus, the decrease of the particle volume during coal burnout insures the particle density against an excessive fall in value unlike other combustion models which hold the constant particle volume.

The particle temperature, T_p, is a solution of the following conservation equation of particle energy [15]

$$\begin{aligned} m_p(t) c_p \frac{dT_p(t)}{dt} &= h^* A_p (T_{f,\infty} - T_p(t)) + \\ A_p \varepsilon_p \sigma\,(T_{f,\infty}^4 - T_p^4(t)) &+ \textstyle\sum_i r_{i,p}(t) \Delta H_i\,, \end{aligned} \tag{48}$$

where h^* is the modified heat transfer coefficient, ΔH_i is the heat of the i-th particle reaction taking place at the rate of $r_{i,p}$. .

The combustion model of pulverized coal, described above, has been implemented into Fluent code by UDFs. Except for the models described above, the mass, momentum and energy conservation equations of the gas phase have been solved by the standard Fluent models. Due to the existing flow conditions inside the reactor, the quantities of the eddy-dissipation model were determined by the transition shear-stress transport turbulence model. The discrete ordinates method was used to solve the radiation transfer equation governing the radiation heat transfer. Although the mean beam length is short in the current laboratory reactor, the modified WSGG model has been adopted and used for oxy combustion [16] while the standard WSGG model was applied for air combustion.

Results and discussion

Figs. 3, 4, and 5, showing contours of selected quantities, give an account of the combustion process in air and oxy-fuel conditions experimentally investigated. Since the model distinguishes between the simultaneous and sequential devolatilization and char combustion separately for small and large coal particles, the smallest particles (with $d_p < 100\mu m$), immediately heated at a high heating rate, simultaneously start devolatilizing and char burning near the burner zone. The burner part arranged inside the reactor gets high temperature so that the small particles flowing near the hot burner walls are easily heated by burner radiation. Unlike the small particles, the large particles (with $d_p > 100\mu m$) first devolatilize, and then the char ignition and combustion occur when their devolatilization is completely finished. Volatile matter released during devolatilization is burnt in a reactor region located upstream to the combustion zone of large char particles.

The gas temperature reaches the highest value of 1550°C for air combustion, and 1332°C and 1412°C for oxy combustion with 25% and 30% O_2, respectively. The oxidation and gasification rates of carbon, presented in g_C/s, show the total rates of adequate reactions.

Fig. 6 compares predicted profiles of selected gas species with experimental points for air and oxy combustion. Except for profiles of the H_2O mole fraction, a reasonable agreement of experimental and predicted data is achieved.

Table 3 presents selected indicators of the NO emission measured during experiments and predicted in numerical simulations. Usually, the NO emission can be expressed using different units, especially mg_{NO}/MJ has been derived from the following expression

$$\overline{\mathrm{NO}} = \frac{\dot{m}_{\mathrm{NO}}}{\dot{m}_c\, Q_c}\,, \qquad (49)$$

where $\dot{m}_{\mathrm{NO}}$ is the NO mass flow rate gained at the reactor outlet, $\dot{m}_c$ is coal mass flow rate supplied to the reactor, Q_c is the coal HHV. However, the practical and true signification of the NO emission is presented by the fuel-N conversion factor expressed in mg_{NO}/mg_{Nf} since it directly provides the NO mass flow rate when the fuel flow rate is ahead known. Comparing NO emission indicators, it is clear that the highest NO emission, expressed in both units of mg_{NO}/MJ and mg_{NO}/mg_{Nf}, is achieved for air combustion due to the impact of thermal NO. Among the oxy combustion cases, the higher NO emission indexes are noted for the higher 30% O_2 mole fraction case comparing with the lower 25% O_2 case. This interesting result can be explained by the higher temperature of 1412 °C reached at 30% O_2 oxy combustion making more favourable oxidizing conditions at which higher amount of NO and higher char burnout can be created.

Finally, the predicted carbon-in-ash (CIA) fraction closely agrees with the experimental one, i.e. 1.60% measured and 4.1% predicted at air combustion, 3.0% measured and 5.0% predicted at oxy combustion with 25% O_2, and 2.70% measured and 2.51% predicted at oxy combustion with 30% O_2.

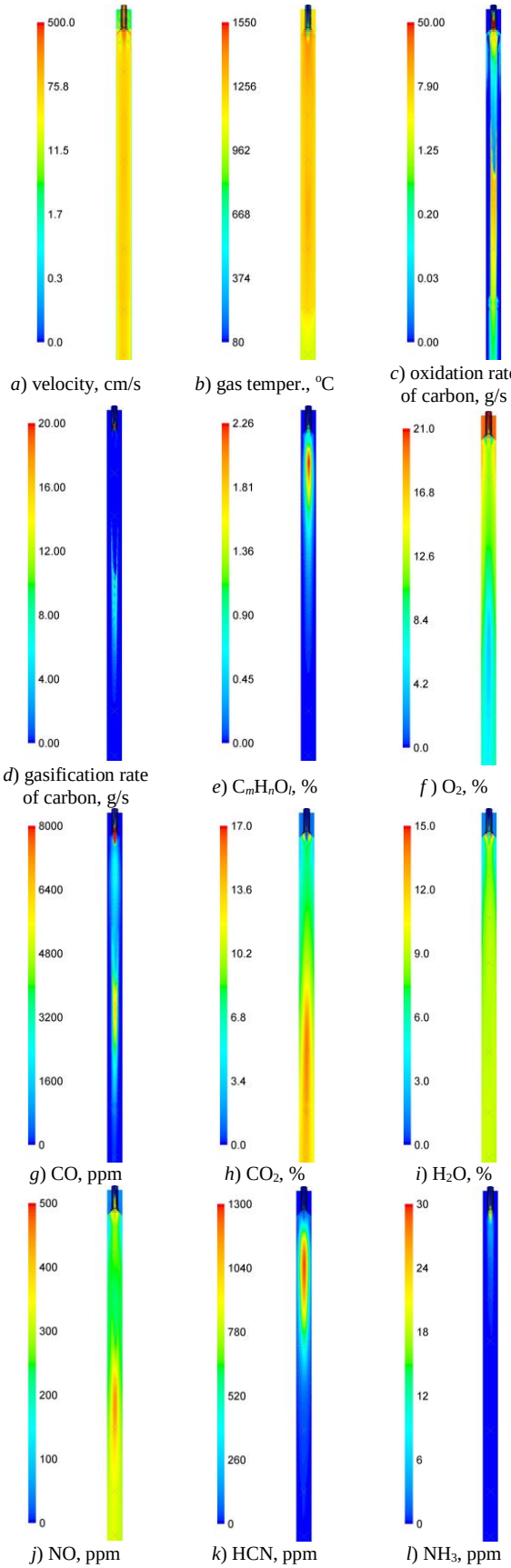

a) velocity, cm/s *b*) gas temper., °C *c*) oxidation rate of carbon, g/s

d) gasification rate of carbon, g/s *e*) $C_mH_nO_l$, % *f*) O_2, %

g) CO, ppm *h*) CO_2, % *i*) H_2O, %

j) NO, ppm *k*) HCN, ppm *l*) NH_3, ppm

Fig. 3: Selected contours showing predicted air combustion of pulverized lignite. × 6 measurement points are located along the reactor axis

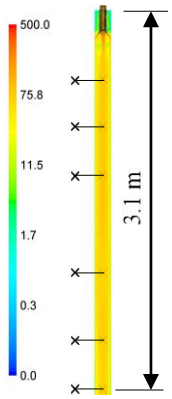

a) velocity, cm/s

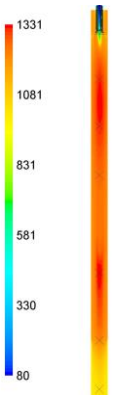

b) gas temp., ^{o}C

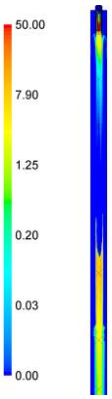

c) oxidation rate of carbon, g/s

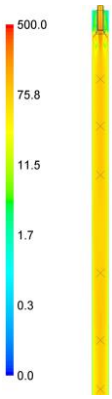

a) velocity, cm/s

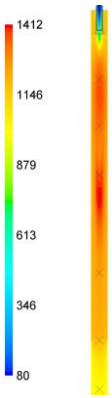

b) gas temp., ^{o}C

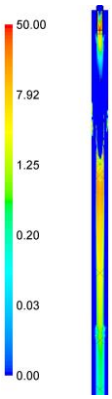

c) oxidation rate of carbon, g/s

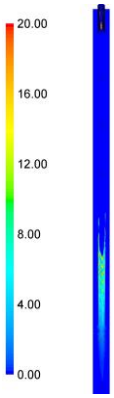

d) gasification rate of carbon, g/s

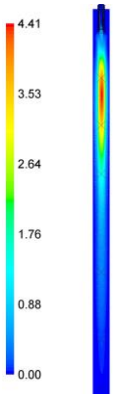

e) $C_mH_nO_l$, %

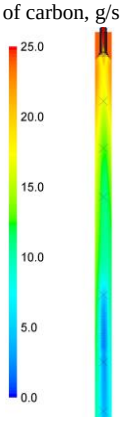

f) O_2, %

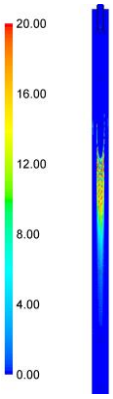

d) gasification rate of carbon,g/s

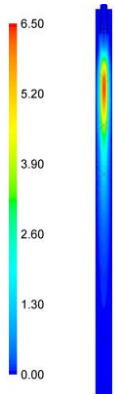

e) $C_mH_nO_l$, %

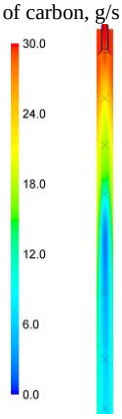

f) O_2, %

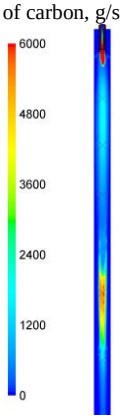

g) CO, ppm

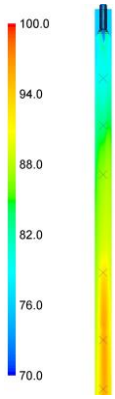

h) CO_2, %

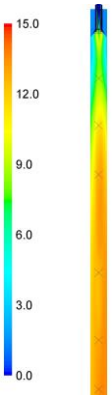

i) H_2O, %

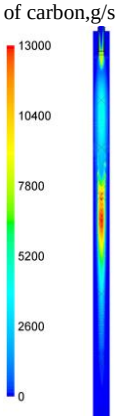

g) CO, ppm

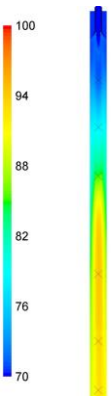

h) CO_2, %

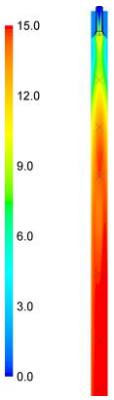

i) H_2O, %

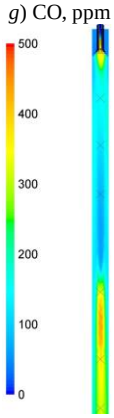

j) NO, ppm

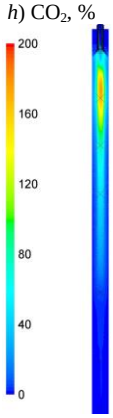

k) HCN, ppm

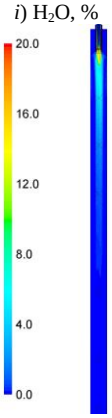

l) NH_3, ppm

Fig. 4: Selected contours showing predicted oxy combustion (25% O_2) of pulverized lignite. × 6 measurement points are located along the reactor axis

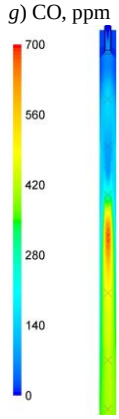

j) NO, ppm

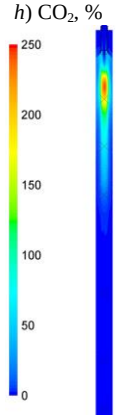

k) HCN, ppm

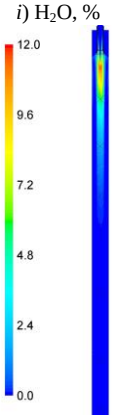

l) NH_3, ppm

Fig. 5: Selected contours showing predicted oxy combustion (30% O_2) of pulverized lignite. × 6 measurement points are located along the reactor axis

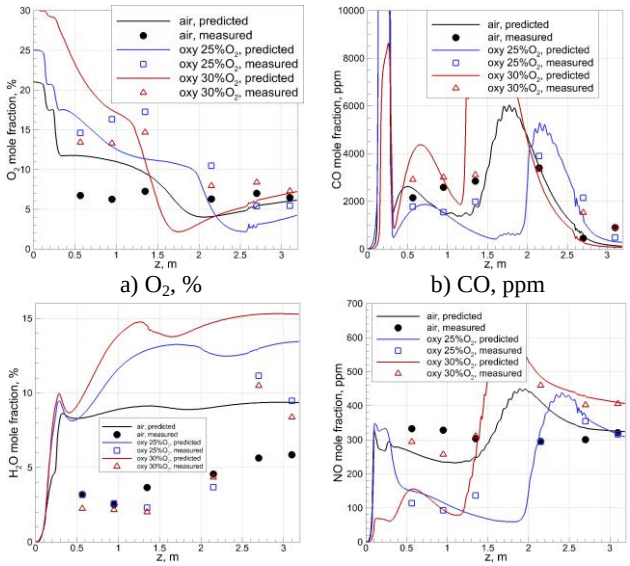

a) O_2, % b) CO, ppm

c) H_2O, % d) NO, ppm

Fig. 6: Measurement points and predicted profiles of species

Table 3: Measured and predicted indicators of the NO emission

combustion in:	measured	predicted from numerical simulation			
	NO ppm, dry	NO ppm dry	mg_{NO}/m^3_n 6%O_2 dry	mg_{NO}/ MJ	mg_{NO}/ mg_{Nf}
air (no thermal NO mechanism)	-	255	345	110	0.499
air (with thermal NO mech.)	321	325	419	138	0.624
oxy, 25% O_2	316	315	372	82.6	0.375
oxy, 30% O_2	406	410	590	106	0.481

Conclusions

First, the laboratory experiments of pulverized lignite combustion were carried out at different conditions of oxy-fuel and air. Essential characteristics of the combustion process were measured, e.g. profiles of main and trace gas species, temperature and char burnout.

Next, a new original combustion model of pulverized coal has been developed. The model considers all important partial processes and phenomena present in pulverized coal combustion. Moreover, a detailed representation of the fuel particle composition has been specially introduced to correctly predict the emission of trace species. Without loss of simplicity making the model easy to use in any CFD computer code, simultaneous changes of particle density and particle size are taken into account by the model and the ignition of char depends on the particle size and the devolatilization level as well.

Finally, a short account of the combustion process was given. The numerical simulations have correctly predicted the combustion behavior in both qualitative and quantitative sense. Different modes of NO_x emission have been successfully explained. The combustion model, verified by the experimental results, has proved its capability to reproduce real combustion conditions even if the operating conditions are only slightly altered so that it is ready-made and can be used in CFD.

Acknowledgements

This scientific work was supported by the National Centre for Research and Development within the confines of Research and Development Strategic Program "*Advanced Technologies for Energy Generation*" project no. 2 "*Oxy–combustion technology for PC and FBC boilers with CO_2 capture*". Agreement no. SP/E/2/66420 /10. The support is gratefully acknowledged.

References

[1] Pawlak-Kruczek H, *et al.*: *The effect of biomass on pollutant emission and burnout in co-combustion with coal*, Combust Sci Tech 187(8), pp. 1511-1539, 2006.

[2] Field M.A., *et al.*: *Combustion of pulverized coal*, Leatherhead, Surrey, Cheney & Sons Ltd., 1967.

[3] Baum M. M., Street P.J.: *Predicting the combustion behaviour of coal particles*, Combust Sci Technol 3(5), pp. 231-243, 1971.

[4] Hercog J., Lewtak R.: *Experimental and numerical investigation of coal char combustion process under standard and oxy-fuel conditions*, Proceedings of the 39th International Technical Conference on Clean Coal & Fuel Systems, Clearwater, USA, 2014.

[5] Biggs M.J, *et al.*: *The CO/CO_2 product ratio for a porous char particle within an incipiently fluidized bed: a numerical study*, Chem Eng Sci 52(6) p.941, 1997.

[6] Magnussen B.F., *et al.*, *Effects of turbulent structure and local concentrations on soot formation and combustion in C_2H_2 diffusion flames*, Symposium (Int.) on Combustion 17(1), pp. 1383-1393, 1979.

[7] Yeoh G.H., Yuen K.K., *Computational fluid dynamics in fire engineering: theory, modelling and practice*, Butterworth-Heinemann, 2009.

[8] Hill S.C., Smoot L.D., *Modeling of nitrogen oxides formation and destruction in combustion systems*, Prog. Energy Combust. Sci. 26, pp. 417-458, 2000.

[9] De Soete G.G., *Overall reaction rates of NO and N_2 formation from fuel nitrogen*, Symposium (Int.) on Combustion 15(1), pp. 1093-1102, 1975.

[10] Chen W., *et al.*, *A computational method for determining global fuel-NO rate expressions. Part 1*, Energy Fuels 10, pp. 1036-1045, 1996.

[11] Xu M., *et al.*, *Modelling of the combustion process and NO_x emission in a utility boiler*, Fuel 79, pp. 1611-1619, 2000.

[12] Chen W, *et al.*: *Global rate expression for nitric oxide reburning. Part 2*, Energy Fuels 10, p1046, 1996.

[13] Smith I.W.: *The combustion rates of coal chars: A review*, Symp (Int.) on Comb 19(1), p. 1045, 1982.

[14] Hamor R.J., *et al.*: *Kinetics of combustion of a pulverized brown coal char between 630 and 2200 K*, Combust Flame 21, pp. 153-162, 1973.

[15] Lewtak R., Milewska A., *Application of different diffusion approaches in oxy-fuel combustion of single coal char particles*, Fuel 113, pp. 844-853, 2013.

[16] Yin C., *et al.*: *New weighted sum of gray gases model applicable to computational fluid dynamics (CFD) modeling of oxy-fuel combustion: derivation, validation, and implementation*, Energy & Fuels 24, p. 6275, 2010.